NAVAL POSTGRADUATE SCHOOL
Monterey, California

THESIS

DYNAMIC CONTROL OF A VEHICLE
WITH
TWO INDEPENDENT WHEELS

by

Douglas R Gerrard

September, 1997

Thesis Advisor:	Xiaoping Yun
Second Reader:	Roberto Cristi

Approved for public release; distribution is unlimited.

19980406 021

DTIC QUALITY INSPECTED 3

REPORT DOCUMENTATION PAGE

Form Approved
OMB No. 0704-0188

Public reporting burden for this collection of information is estimated to average 1 hour per response, including the time for reviewing instruction, searching existing data sources, gathering and maintaining the data needed, and completing and reviewing the collection of information. Send comments regarding this burden estimate or any other aspect of this collection of information, including suggestions for reducing this burden, to Washington headquarters Services, Directorate for Information Operations and Reports, 1215 Jefferson Davis Highway, Suite 1204, Arlington, VA 22202-4302, and to the Office of Management and Budget, Paperwork Reduction Project (0704-0188) Washington DC 20503.

1. AGENCY USE ONLY ***(Leave blank)***	**2. REPORT DATE** September 1997	**3. REPORT TYPE AND DATES COVERED** Master's Thesis

4. TITLE AND SUBTITLE
DYNAMIC CONTROL OF A VEHICLE WITH TWO INDEPENDENT WHEELS

5. FUNDING NUMBERS

6. AUTHOR(S)
Gerrard, Douglas R.

7. PERFORMING ORGANIZATION NAME(S) AND ADDRESS(ES)
Naval Postgraduate School
Monterey, CA 93943-5000

8. PERFORMING ORGANIZATION REPORT NUMBER

9. SPONSORING / MONITORING AGENCY NAME(S) AND ADDRESS(ES)

10. SPONSORING / MONITORING AGENCY REPORT NUMBER

11. SUPPLEMENTARY NOTES

The views expressed in this thesis are those of the author and do not reflect the official policy or position of the Department of Defense or the U.S. Government.

12a. DISTRIBUTION / AVAILABILITY STATEMENT
Approved for public release; distribution is unlimited.

12b. DISTRIBUTION CODE

13. ABSTRACT *(maximum 200 words)*

The feedback control and modeling of a mobile robot with two wheels that are independently steerable and drivable is studied. Two-wheel steer vehicles increase their maneuverability when both wheels are powered and therefore increases their performance in confined spaces. A dynamic feedback control algorithm is developed, which enables the vehicle to move from any initial configuration (position and orientation) to any final configuration. Simulation results are presented to verify the independent control of the two position variables and the orientation variable. A comparison with a two-wheel steering and one wheel drive vehicle shows that driving both wheels increases performance and maneuverability.

14. SUBJECT TERMS
Two Wheel Steer, Two Wheel Drivable Vehicle, Dynamic Feedback Control Algorithm, Highly Maneuverable Vehicle

15. NUMBER OF PAGES
38

16. PRICE CODE

17. SECURITY CLASSIFICATION OF REPORT Unclassified	**18. SECURITY CLASSIFICATION OF THIS PAGE** Unclassified	**19. SECURITY CLASSIFI- CATION OF ABSTRACT** Unclassified	**20. LIMITATION OF ABSTRACT** UL

NSN 7540-01-280-5500

Standard Form 298 (Rev. 2-89)
Prescribed by ANSI Std. 239-18

Approved for public release; distribution is unlimited

DYNAMIC CONTROL OF A VEHICLE WITH TWO INDEPENDENT WHEELS

Douglas R. Gerrard
Lieutenant, United States Navy
B.S., University of Missouri, 1990

Submitted in partial fulfillment of the
requirements for the degree of

MASTER OF SCIENCE IN ELECTRICAL ENGINEERING

from the

NAVAL POSTGRADUATE SCHOOL
September 1997

Author: Douglas R Gerrard
Douglas R. Gerrard

Approved by:
Xiaoping Yun, Thesis Advisor

Roberto Cristi, Second Reader

Herschel H. Loomis, Jr., Chairman
Department of Electrical & Computer Engineering

ABSTRACT

The feedback control and modeling of a mobile robot with two wheels that are independently steerable and drivable is studied. Two-wheel steer vehicles increase their maneuverability when both wheels are drivable and therefore increases their performance in confined spaces. A dynamic feedback control algorithm is developed, which enables the vehicle to move from any initial configuration (position and orientation) to any final configuration. Simulation results are presented to verify the independent control of the two position variables and the orientation variable. A comparison with a two-wheel steering and one wheel drive vehicle shows that driving both wheels increases performance and maneuverability.

TABLE OF CONTENTS

I. INTRODUCTION 1

II. KINEMATIC MODEL OF THE VEHICLE 3

A. NOTATIONS 3
B. VELOCITY KINEMATICS 4
C. CONSTRAINT EQUATIONS 5
D. KINEMATIC MODEL 6
E. DYNAMICS 8

III. FEEDBACK CONTROL 11

A. STATIC FEEDBACK 11
B. DYNAMIC FEEDBACK 12

IV. SIMULATION 15

A. TEST CONDITIONS 15
B. INDEPENDENT CONTROL OF POSITION AND ORIENTATION 17
C. ONE WHEEL VERSUS TWO WHEEL DRIVABLE VEHICLES 22

V. CONCLUSION AND FUTURE WORK 25

LIST OF REFERENCES 27

INITIAL DISTRIBUTION LIST 29

I. INTRODUCTION

Wheeled mobile robots come in a number of different kinematic structures. Typical robots have a steerable front wheel(s), and the rear wheel(s) whose orientation relative to the vehicle body is fixed, such as an automobile or a bicycle. Some robots are the differential-drive type which have two co-axial wheels that are independently actuated to achieve forward/backward and rotational motions. The synchronous-drive type of mobile robots such as Nomad 200 [Ref. 1] have all the wheels steer and rotate together so that the wheels are parallel all the time. Mobile robots such as these have two degrees of freedom and are nonholonomically constrained.

This thesis describes a type of mobile robot that has two independently steerable and drivable wheels. Using the bicycle as an example, this type of mobile robot would have both the front and rear wheels drivable as well as steerable. It has been shown that a mobile vehicle with two steerable wheels with one drivable can be controlled using dynamic feedback control [Ref. 2]. One example of this type of mobile robot is the SR2 mobile robot from Cybermotion Inc. which has three steerable and drivable wheels [Ref. 3]. Four-wheel steering automobiles [Ref. 4 and Ref. 5] and fire trucks [Ref. 6] are other examples, both of which are designed for improving maneuverability. Although these types of vehicles are still nonholonomically constrained, they can still be controlled to follow a path with independent orientation [Ref. 7] and are extremely maneuverable in confined space [Ref. 8].

This thesis focuses on modeling and control of a vehicle with two wheels, both of which are steerable and drivable. The vehicle has four input variables, the steering velocities of the two wheels and the rotational velocity of both wheels. The problem of how to steer and deliver the torque to the two wheels in order to independently control the position and orientation of the vehicle body is studied. In particular, a dynamic feedback algorithm is developed, which linearizes and decouples the system. The output in this case is the two-dimensional position and one-dimensional orientation of the vehicle body.

Consequently, the algorithm enables the vehicle to follow any desired position trajectory and orientation trajectory. Furthermore, it will be shown that the input-output linearization cannot be achieved by any static state feedback [Ref. 2]. Dynamic feedback linearization was previously applied to three-wheel mobile robots (with a free or steering wheel) that have only two inputs [Ref. 9].

One of the benefits of having both wheels drivable would include increasing the maneuverability the vehicle. Both wheels drivable would allow pure rotation in place and pure translation in the lateral direction of the vehicle. Imagine parallel parking by just rotating all wheels perpendicular to the body of the vehicle and laterally translating into the parking space. Another benefit would be the ability to have the torque distributed to the wheels depending on the road conditions, and if a wheel began to slip, the torque delivered to the wheels could be transferred to the other wheel. This would result in a two wheel steerable, one wheel drivable vehicle until the slipping wheel regains traction.

II. KINEMATIC MODEL OF THE VEHICLE

A. NOTATIONS

Figure 1 shows a diagram of a vehicle with two independent steering wheels. The two wheels are located at p_1 and p_2 on the vehicle, respectively. p_0 is located at the center of gravity of the vehicle which is assumed to be located on the p_1 - p_2 axis. The distance from p_0 to p_1 is **a** and the distance from p_0 to p_2 is **b**.

Four coordinate frames are defined for describing position and orientation of the vehicle [Ref. 2]. {U} is the earth-fixed coordinate frame. {1} is the frame fixed on wheel 1. x_1 is chosen to be along the horizontal radial direction and y_1 is in the lateral direction. Likewise, {2} is the frame defined for wheel 2. {0} is the frame defined at point p_0. y_0 is chosen to be a unit vector pointing from p_2 to p_1, and x_0 is orthogonal to the line segment from p_2 to p_1.

The orientation of the vehicle body is characterized by ϕ_o, which is the angle from x_U to x_0. ϕ_1 and ϕ_2 are two steering angles defined from x_0 to x_i, $i = 1,2$. With these

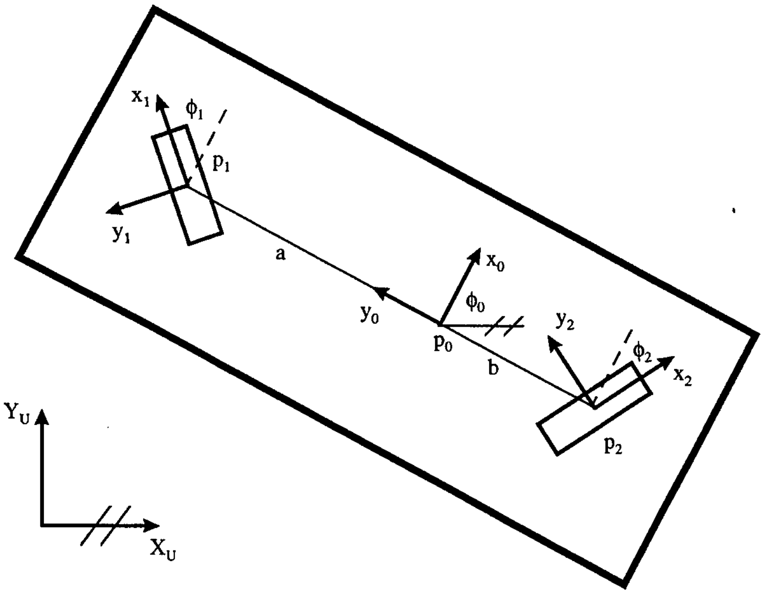

Figure 1: Coordinate systems for a two steering wheel vehicle

notations, we are ready to establish homogeneous transformations describing one frame relative to another. In what follows, ${}^{a}_{b}T$ denotes the homogeneous transformation of frame {b} relative to frame {a}. Because the motion of the vehicle is restricted to the two-dimensional plane, homogeneous transformations are 3 x 3 rather than 4 x 4.

$${}^{U}_{0}T = \begin{bmatrix} \cos(\phi_0) & -\sin(\phi_0) & x_0 \\ \sin(\phi_0) & \cos(\phi_0) & y_0 \\ 0 & 0 & 1 \end{bmatrix}$$

$${}^{0}_{1}T = \begin{bmatrix} \cos(\phi_1) & -\sin(\phi_1) & 0 \\ \sin(\phi_1) & \cos(\phi_1) & a \\ 0 & 0 & 1 \end{bmatrix}$$

$${}^{0}_{2}T = \begin{bmatrix} \cos(\phi_2) & -\sin(\phi_2) & 0 \\ \sin(\phi_2) & \cos(\phi_2) & -b \\ 0 & 0 & 1 \end{bmatrix}$$

B. VELOCITY KINEMATICS

With the help of homogeneous transformations given above, the velocities of point p_1 and point p_2 can be computed. The homogeneous position vector of point p_1 and p_2 expressed in frame {0} are:

$${}^{0}p_1 = \begin{bmatrix} 0 \\ a \\ 1 \end{bmatrix} \qquad {}^{0}p_2 = \begin{bmatrix} 0 \\ -b \\ 1 \end{bmatrix}$$

These points are represented in frame {U} by

$${}^{U}p_1 = {}^{U}_{0}T\,{}^{0}p_1 = \begin{bmatrix} \cos(\phi_0) & -\sin(\phi_0) & x_0 \\ \sin(\phi_0) & \cos(\phi_0) & y_0 \\ 0 & 0 & 1 \end{bmatrix} \begin{bmatrix} 0 \\ a \\ 1 \end{bmatrix} = \begin{bmatrix} -a\sin(\phi_0) + x_0 \\ a\cos(\phi_0) + y_0 \\ 1 \end{bmatrix}$$

$${}^{U}p_2 = {}^{U}_{0}T\,{}^{0}p_2 = \begin{bmatrix} \cos(\phi_0) & -\sin(\phi_0) & x_0 \\ \sin(\phi_0) & \cos(\phi_0) & y_0 \\ 0 & 0 & 1 \end{bmatrix} \begin{bmatrix} 0 \\ -b \\ 1 \end{bmatrix} = \begin{bmatrix} b\sin(\phi_0) + x_0 \\ -b\cos(\phi_0) + y_0 \\ 1 \end{bmatrix}$$

The velocity of the points p$_1$ and p$_2$ (or differentiated with respect to frame $\{U\}$) expressed in frame $\{U\}$ are:

$$ {}^U\dot{p}_1 = \begin{bmatrix} -a\cos(\phi_0)\dot{\phi}_0 + \dot{x}_0 \\ -a\sin(\phi_0)\dot{\phi}_0 + \dot{y}_0 \\ 0 \end{bmatrix} \qquad {}^U\dot{p}_2 = \begin{bmatrix} b\cos(\phi_0)\dot{\phi}_0 + \dot{x}_0 \\ b\sin(\phi_0)\dot{\phi}_0 + \dot{y}_0 \\ 0 \end{bmatrix} $$

In order to derive the nonholonomic constraint equations of wheel 1, the velocity of point p$_1$ relative to frame $\{U\}$ is expressed in frame $\{1\}$:

$$ {}^1\dot{p}_1 = \left({}^U_1T\right)^{-1}\,{}^U\dot{p}_1 = \left({}^U_0T\,{}^0_1T\right)^{-1}\,{}^U\dot{p}_1 = \begin{bmatrix} \cos(\phi_0+\phi_1) & \sin(\phi_0+\phi_1) & * \\ -\sin(\phi_0+\phi_1) & \cos(\phi_0+\phi_1) & * \\ 0 & 0 & 1 \end{bmatrix} {}^U\dot{p}_1 = $$

$$ \begin{bmatrix} \dot{x}_0\cos(\phi_0+\phi_1) + \dot{y}_0\sin(\phi_0+\phi_1) - a\dot{\phi}_0\cos(\phi_1) \\ -\dot{x}_0\sin(\phi_0+\phi_1) + \dot{y}_0\cos(\phi_0+\phi_1) + a\dot{\phi}_0\sin(\phi_1) \\ 0 \end{bmatrix} $$

where the terms indicated by * are irrelevant in the computation. Likewise, the velocity of point 2 relative to frame $\{U\}$ is expressed in frame $\{2\}$ as follows:

$$ {}^2\dot{p}_2 = \begin{bmatrix} \dot{x}_0\cos(\phi_0+\phi_2) + \dot{y}_0\sin(\phi_0+\phi_2) + b\dot{\phi}_0\cos(\phi_2) \\ -\dot{x}_0\sin(\phi_0+\phi_2) + \dot{y}_0\cos(\phi_0+\phi_2) - b\dot{\phi}_0\sin(\phi_2) \\ 0 \end{bmatrix} $$

C. CONSTRAINT EQUATIONS

The vehicle is subjected to four nonholonomic constraints. The first two constraints are derived from the fact that the wheels cannot move in the lateral direction. That is, the **y** component of ${}^1\dot{p}_1$ and ${}^2\dot{p}_2$ is zero:

$$ -\dot{x}_0\sin(\phi_0+\phi_1) + \dot{y}_0\cos(\phi_0+\phi_1) + a\dot{\phi}_0\sin(\phi_1) = 0 $$

$$ -\dot{x}_0\sin(\phi_0+\phi_2) + \dot{y}_0\cos(\phi_0+\phi_2) - b\dot{\phi}_0\sin(\phi_2) = 0 $$

The other two constraints are due to the no-slip condition. Let r be the radius of the wheels, and θ_i, i=1,2 be the angular displacement of the wheels (driving angles) then the **x** component of ${}^{1}\dot{p}_1$ and ${}^{2}\dot{p}_2$ is equal to the velocity of the wheel in that direction. These two constraints are expressed as:

$$\dot{x}_0 \cos(\phi_0 + \phi_1) + \dot{y}_0 \sin(\phi_0 + \phi_1) - a\dot{\phi}_0 \cos(\phi_1) = r\dot{\theta}_1$$

$$\dot{x}_0 \cos(\phi_0 + \phi_2) + \dot{y}_0 \sin(\phi_0 + \phi_2) + b\dot{\phi}_0 \cos(\phi_2) = r\dot{\theta}_2$$

Choosing the following generalized coordinate vector

$$q = \begin{bmatrix} x_0 & y_0 & \theta_1 & \theta_2 & \phi_0 & \phi_1 & \phi_2 \end{bmatrix}^T$$

the four constraints can be written as

$$A(q)\dot{q} = 0 \tag{1}$$

where the 4 x 7 dimensional matrix A(q) is given by

$$A(q) = \begin{bmatrix} -\sin(\phi_0 + \phi_1) & \cos(\phi_0 + \phi_1) & 0 & 0 & a\sin(\phi_1) & 0 & 0 \\ -\sin(\phi_0 + \phi_2) & \cos(\phi_0 + \phi_2) & 0 & 0 & -b\sin(\phi_2) & 0 & 0 \\ \cos(\phi_0 + \phi_1) & \sin(\phi_0 + \phi_1) & -r & 0 & -a\cos(\phi_1) & 0 & 0 \\ \cos(\phi_0 + \phi_2) & \sin(\phi_0 + \phi_2) & 0 & -r & b\cos(\phi_2) & 0 & 0 \end{bmatrix}$$

D. KINEMATIC MODEL

The 4 x 7 dimensional matrix A(q) has a 3-dimensional null space. Let

$$S(q) = \begin{bmatrix} s_1(q) & s_2(q) & s_3(q) \end{bmatrix}$$

be a 7 x 3 full-rank matrix whose columns $s_i(q)$, i=1,2,3, are in the null space of A(q), that is, A(q) $s_i(q) = 0$. The three columns of S(q) form a basis for the null space of A(q). Since the generalized velocity $\dot{q}$ is always in the null space of A(q) as characterized by Equation (1), it may be expressed as

$$\dot{q} = S(q)\eta \tag{2}$$

where η is a 3-dimensional vector of independent velocities. It is noted that the choice of S(q) and the corresponding η is not unique. For a certain choice, η may not necessarily represent any physical velocity.

As stated earlier, both wheels are steerable and powered. However, only three velocity inputs are needed. If we choose η to be the three angular input velocities, that is,

$$\eta = \begin{bmatrix} \eta_1 \\ \eta_2 \\ \eta_3 \end{bmatrix} = \begin{bmatrix} \dot{\theta}_1 \\ \dot{\phi}_1 \\ \dot{\phi}_2 \end{bmatrix} \tag{3}$$

the corresponding S(q) is then given by

$$S(q) = \begin{bmatrix} s_{11}(q) & 0 & 0 \\ s_{21}(q) & 0 & 0 \\ 1 & 0 & 0 \\ s_{41}(q) & 0 & 0 \\ s_{51}(q) & 0 & 0 \\ 0 & 1 & 0 \\ 0 & 0 & 1 \end{bmatrix}$$

where

$$s_{11}(q) = r\left[\cos(\phi_0 + \phi_1) - \frac{\cos\phi_0 \sin(\phi_2 - \phi_1)}{2\sin\phi_2}\right]$$

$$s_{21}(q) = r\left[\sin(\phi_0 + \phi_1) - \frac{\sin\phi_0 \sin(\phi_2 - \phi_1)}{2\sin\phi_2}\right]$$

$$s_{41}(q) = \frac{\sin\phi_1}{\sin\phi_2}$$

$$s_{51}(q) = -\frac{r}{(a+b)}\frac{\sin(\phi_2 - \phi_1)}{\sin\phi_2}$$

E. DYNAMICS

Since only one wheel rotation velocity is used as one of the inputs, the torque delivered to both wheels must be incorporated into this single input. This relationship is obtained by solving the dynamic equation for the forces. Figure 2 shows the dynamic forces acting on the body and wheel unit. Summing the moments about the z_0 axis at the center of gravity yields

$$\sum M_{z_0} = -aF_1 \cos\phi_1 + bF_2 \cos\phi_2 = I_B \ddot{\phi}_0 \tag{4}$$

where I_B is the body moment of inertia. For the wheel, summing the moments at the point where wheel i, (i = 1,2) makes contact with the surface yields

$$\sum M_z = cF_i + \tau_i = I_W \ddot{\theta}_i + rm_W a_i$$

where I_W is the wheel moment of inertia and m_W is the mass of the wheel. Since the acceleration $a_i = r\ddot{\theta}_i$,

$$F_i = \frac{-\tau_i + \ddot{\theta}_i\left(I_W + r^2 m_W\right)}{c}. \tag{5}$$

Combining Equation (4) and Equation (5) provide the governing equation of motion.

$$a\tau_1 \cos\phi_1 - b\tau_2 \cos\phi_2 - a\bar{I}_W \ddot{\theta}_1 \cos\phi_1 + b\bar{I}_W \ddot{\theta}_2 \cos\phi_2 = cI_B \ddot{\phi}_0 \tag{6}$$

where $\bar{I}_W = I_W + r^2 m_W$.

From Figure 3, the following relationships can be derived. The velocity diagram and the law of sine's provide the following relationship between $\dot{\theta}_1$ and $\dot{\theta}_2$.

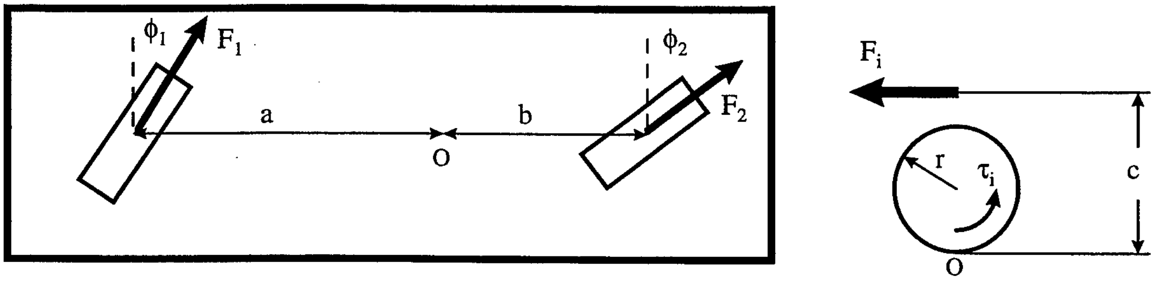

Figure 2: Dynamic force diagram

$$\frac{\sin\phi_1}{L_2}=\frac{\sin\phi_2}{L_1}=\frac{\sin(\phi_2-\phi_1)}{a+b}$$

$$\dot{\phi}_0=\frac{V_1}{L_1}=\frac{V_2}{L_2}=-\frac{r\dot{\theta}_2\sin(\phi_2-\phi_1)}{\sin\phi_1(a+b)}=-\frac{r\dot{\theta}_1\sin(\phi_2-\phi_1)}{\sin\phi_2(a+b)} \tag{7}$$

$$\dot{\theta}_1\sin\phi_1=\dot{\theta}_2\sin\phi_2 \tag{8}$$

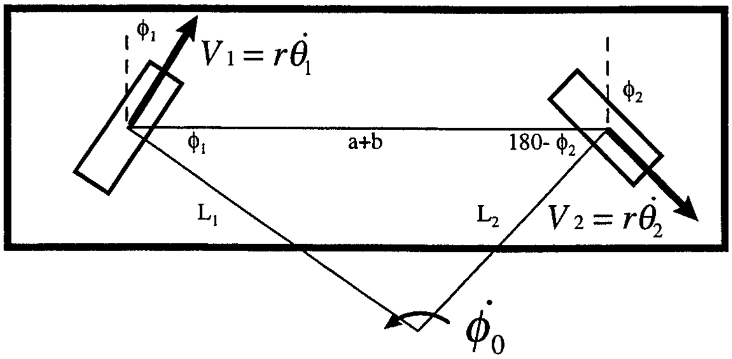

Figure 3: Kinematic velocity diagram

Differentiating Equation (7) and Equation (8) and making substitutions and solving for $\ddot{\theta}_2$ provide

$$\ddot{\theta}_2=\frac{\ddot{\theta}_1\sin\phi_1\sin(\phi_2-\phi_1)+\dot{\phi}_0\left[\dot{\phi}_2(a+b)\sin\phi_1\cos\phi_2-\dot{\phi}_1(a+b)\cos\phi_1\sin\phi_2\right]}{r\sin\phi_2\sin(\phi_2-\phi_1)} \tag{9}$$

Likewise, solving for $\ddot{\phi}_0$

$$\ddot{\phi}_0=\frac{-\ddot{\theta}_1 r\sin^2(\phi_2-\phi_1)+\dot{\phi}_0(a+b)\left[\sin\phi_2\cos(\phi_2-\phi_1)(\dot{\phi}_2-\dot{\phi}_1)+\dot{\phi}_2\cos\phi_2\sin(\phi_2-\phi_1)\right]}{(a+b)\sin\phi_2\sin(\phi_2-\phi_1)} \tag{10}$$

Combining Equation (6), Equation (9), and Equation (10) gives the equation for the angular acceleration of wheel 1 as a function of both wheels input torque and the angular velocity of the body.

$$
\begin{aligned}
&\ddot{\theta}_1 r \sin(\phi_2 - \phi_1)\left[a\bar{I}_W (a+b)\cos\phi_1 \sin\phi_2 - b\bar{I}_W (a+b)\sin\phi_1 \cos\phi_2 - cI_B r \sin(\phi_2 - \phi_1)\right] = \\
&\quad \tau_1\left[ar(a+b)\cos\phi_1 \sin\phi_2 \sin(\phi_2 - \phi_1)\right] - \tau_2\left[br(a+b)\cos\phi_2 \sin\phi_2 \sin(\phi_2 - \phi_1)\right] \\
&\quad + \dot{\phi}_0 \begin{bmatrix} b\bar{I}_W (a+b)^2 \cos\phi_2\left[\dot{\phi}_2 \sin\phi_1 \cos\phi_2 - \dot{\phi}_1 \cos\phi_1 \sin\phi_2\right] \\ - cI_B r(a+b)\left[\sin\phi_2 \cos(\phi_2 - \phi_1)(\dot{\phi}_2 - \dot{\phi}_1) - \dot{\phi}_2 \cos\phi_2 \sin(\phi_2 - \phi_1)\right] \end{bmatrix} \qquad (11)
\end{aligned}
$$

Equation (11) can be integrated to provide the angular velocity of wheel 1 for the input to the control algorithm. In this way, both torque inputs are combined into a single input necessary for use as one of the three inputs for the control algorithm. The other two inputs will be the two steering angular velocities.

The next chapter develops the control for the vehicle and uses these three velocities as the inputs for the feedback control algorithm. From these three inputs to the control algorithm, the seven dimensional state vector provides the outputs of the vehicle's position and orientation.

III. FEEDBACK CONTROL

Considering the generalized coordinate vector q as the state vector, the kinematic model of the vehicle represented in the state space form is characterized by Equation (2) in which η is the input to the system. To control the position and orientation of the vehicle, the natural choice for the output equation is:

$$y = h(q) = \begin{bmatrix} x_0 \\ y_0 \\ \phi_0 \end{bmatrix}$$

Once the state equation and output equation are derived, the next step is to design a controller for this system. Feedback linearization technique is used [Ref. 10]. It has been shown that a static feedback is not capable of linearizing the system [Ref. 2] which will be repeated here. Furthermore, the dynamic feedback that linearizes and decouples the system will also be derived.

A. STATIC FEEDBACK

To derive a static nonlinear feedback, we differentiate the output equation.

$$\dot{y} = \frac{\partial h(q)}{\partial q}\dot{q} = \frac{\partial h(q)}{\partial q}S(q)\eta = \Phi(q)\eta$$

where $\Phi(q)$ denotes the decoupling matrix of the system. If $\Phi(q)$ is of full rank, we may apply a static feedback of the form

$$\eta = \Phi^{-1}(q)\mu$$

to obtain the linearized closed-loop system:

$$\dot{y} = \mu$$

In the present case, the decoupling matrix is given by

$$\Phi(q) = \frac{\partial h(q)}{\partial q}S(q) = \begin{bmatrix} s_{11}(q) & 0 & 0 \\ s_{21}(q) & 0 & 0 \\ s_{51}(q) & 0 & 0 \end{bmatrix}$$

which is unfortunately singular. Therefore, it is not possible to have a static feedback that linearizes the system.

B. DYNAMIC FEEDBACK

If a system is not linearizable by any static feedback, it may nevertheless be linearizable by a dynamic feedback. The construction of a dynamic feedback consists of two steps. First we construct a static feedback shown below, which is called Feedback I:

$$\eta = \begin{bmatrix} s_{11}^{-1}(q) & 0 & 0 \\ 0 & 1 & 0 \\ 0 & 0 & 1 \end{bmatrix} \mu$$

The application of this feedback results in the following closed-loop system:

$$\dot{y} = \mu_1$$

$$\begin{bmatrix} \dot{y}_2 \\ \dot{y}_3 \end{bmatrix} = \begin{bmatrix} s_{21}/s_{11} \\ s_{51}/s_{11} \end{bmatrix} \mu_1 = \begin{bmatrix} \Psi_{11}(\phi_0, \phi_1, \phi_2) \\ \Psi_{21}(\phi_0, \phi_1, \phi_2) \end{bmatrix} \mu_1$$

It is noted that the first component of the output is linearized and decoupled from the other two components. Next, we apply another feedback in order to linearize the latter two components of the output. To do so, we differentiate them once more.

$$\begin{bmatrix} \ddot{y}_2 \\ \ddot{y}_3 \end{bmatrix} = \begin{bmatrix} \Psi_{11} \\ \Psi_{21} \end{bmatrix} \dot{\mu}_1 + \mu_1 \begin{bmatrix} \dfrac{\partial \Psi_{11}}{\partial \phi_0} \\ \dfrac{\partial \Psi_{21}}{\partial \phi_0} \end{bmatrix} \dot{\phi}_0 + \mu_1 \begin{bmatrix} \dfrac{\partial \Psi_{11}}{\partial \phi_1} & \dfrac{\partial \Psi_{11}}{\partial \phi_2} \\ \dfrac{\partial \Psi_{21}}{\partial \phi_1} & \dfrac{\partial \Psi_{21}}{\partial \phi_2} \end{bmatrix} \begin{bmatrix} \dot{\phi}_1 \\ \dot{\phi}_2 \end{bmatrix}$$

Noting that $\dot{\phi}_0 = s_{51}\eta_1 = s_{51}/s_{11}\,\mu_1$, and

$$\begin{bmatrix} \dot{\phi}_1 \\ \dot{\phi}_2 \end{bmatrix} = \begin{bmatrix} \eta_2 \\ \eta_3 \end{bmatrix} = \begin{bmatrix} \mu_2 \\ \mu_3 \end{bmatrix}$$

we may represent the above equation as follows:

$$\begin{bmatrix} \ddot{y}_2 \\ \ddot{y}_3 \end{bmatrix} = Q_1(q)\dot{\mu}_1 + Q_2(q)\mu_1^2 + \Omega(q) \begin{bmatrix} \mu_2 \\ \mu_3 \end{bmatrix}$$

where

$$\begin{bmatrix} \ddot{y}_2 \\ \ddot{y}_3 \end{bmatrix} = Q_1(q)\dot{\mu}_1 + Q_2(q)\mu_1^2 + \Omega(q)\begin{bmatrix} \mu_2 \\ \mu_3 \end{bmatrix}$$

where

$$Q_1(q) = \begin{bmatrix} \Psi_{11} \\ \Psi_{21} \end{bmatrix}$$

$$Q_2(q) = \begin{bmatrix} \dfrac{\partial \Psi_{11}}{\partial \phi_0} \\ \dfrac{\partial \Psi_{21}}{\partial \phi_0} \end{bmatrix} s_{51}/s_{11}$$

$$\Omega(q) = \mu_1 \begin{bmatrix} \dfrac{\partial \Psi_{11}}{\partial \phi_1} & \dfrac{\partial \Psi_{11}}{\partial \phi_2} \\ \dfrac{\partial \Psi_{21}}{\partial \phi_1} & \dfrac{\partial \Psi_{21}}{\partial \phi_2} \end{bmatrix}$$

Now applying Feedback II given by

$$\begin{bmatrix} \mu_2 \\ \mu_3 \end{bmatrix} = \Omega^{-1}(q)\left(\begin{bmatrix} v_2 \\ v_3 \end{bmatrix} - Q_1(q)\dot{\mu}_1 - Q_2(q)\mu_1^2\right)$$

the latter two outputs are linearized as

$$\begin{bmatrix} \ddot{y}_2 \\ \ddot{y}_3 \end{bmatrix} = \begin{bmatrix} v_2 \\ v_3 \end{bmatrix}$$

Furthermore, let $\dot{\mu}_1 = v_1$, therefore

$$\ddot{y}_1 = v_1$$

The complete controller with three feedback loops for the steering angles and the wheel velocity input is depicted in a block diagram in Figure 4. Figure 5 shows the MATLAB Simulink program diagram.

The simulation results are provided in the next chapter. The results showed a significant improvement in performance over the two-wheel steerable, one-wheel drivable vehicle.

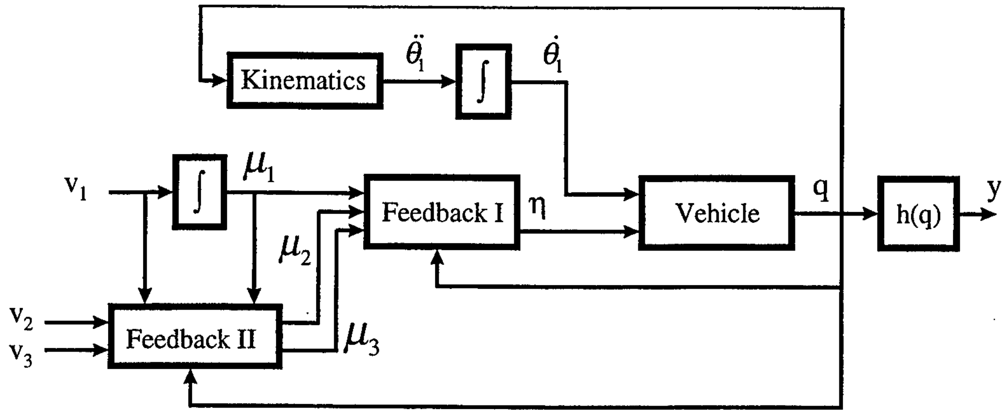
Kinematics
$\ddot{\theta}_1$
$\int$
$\dot{\theta}_1$
v_1
$\int$
μ_1
Feedback I
η
Vehicle
q
h(q)
y
μ_2
v_2
v_3
Feedback II
μ_3

Figure 4: Dynamic feedback controller

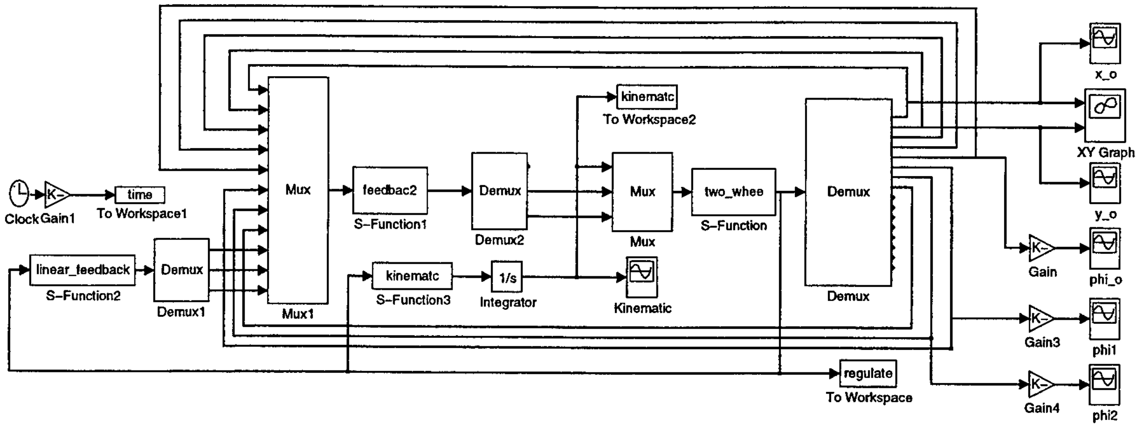
Clock
Gain1
K-
time
To Workspace1
linear_feedback
S-Function2
Demux
Demux1
Mux
Mux1
feedbac2
S-Function1
Demux
Demux2
kinematc
S-Function3
1/s
Integrator
kinematc
To Workspace2
Mux
Mux
Kinematic
two_whee
S-Function
Demux
Demux
regulate
To Workspace
x_o
XY Graph
y_o
K-
Gain
phi_o
K-
Gain3
phi1
K-
Gain4
phi2

Figure 5: MATLAB Simulink program

IV. SIMULATION

A. TEST CONDITIONS

The vehicle feedback control system shown in Figure 4 has been simulated using Matlab Simulink (Figure 5). Each block in the figure is implemented by the use of an S-function [Ref. 11]. To stabilize each of the linearized subsystems, the linear feedback is further designed. In the simulation, the linear feedback gain is chosen to place the poles of each subsystem at -5 and -15. The system was tested and compared to the performance of the dynamic control algorithm for the two steering, one wheel drivable vehicle. The following are the initial and goal configurations used for the test:

$$\begin{bmatrix} x_0 \\ y_0 \\ \phi_0 \end{bmatrix}_{init} = \begin{bmatrix} 0 \\ 0 \\ 50^\circ \end{bmatrix} \qquad \begin{bmatrix} x_0 \\ y_0 \\ \phi_0 \end{bmatrix}_{goal} = \begin{bmatrix} 10 \\ -5 \\ -10^\circ \end{bmatrix}$$

The parameters used for the simulation are designed to be realistic of an actual robot and in MKS units and are as follows:

$$a = 0.55 \qquad b = 0.30 \qquad c = 0.25$$

$$r = 0.10 \qquad I_B = 2.0 \qquad \bar{I}_W = 0.05$$

Figure 6 clearly shows that the path from the initial point to the goal is a straight line. This direct path was the result for the two steering wheel vehicle regardless if one or both wheels were powered.

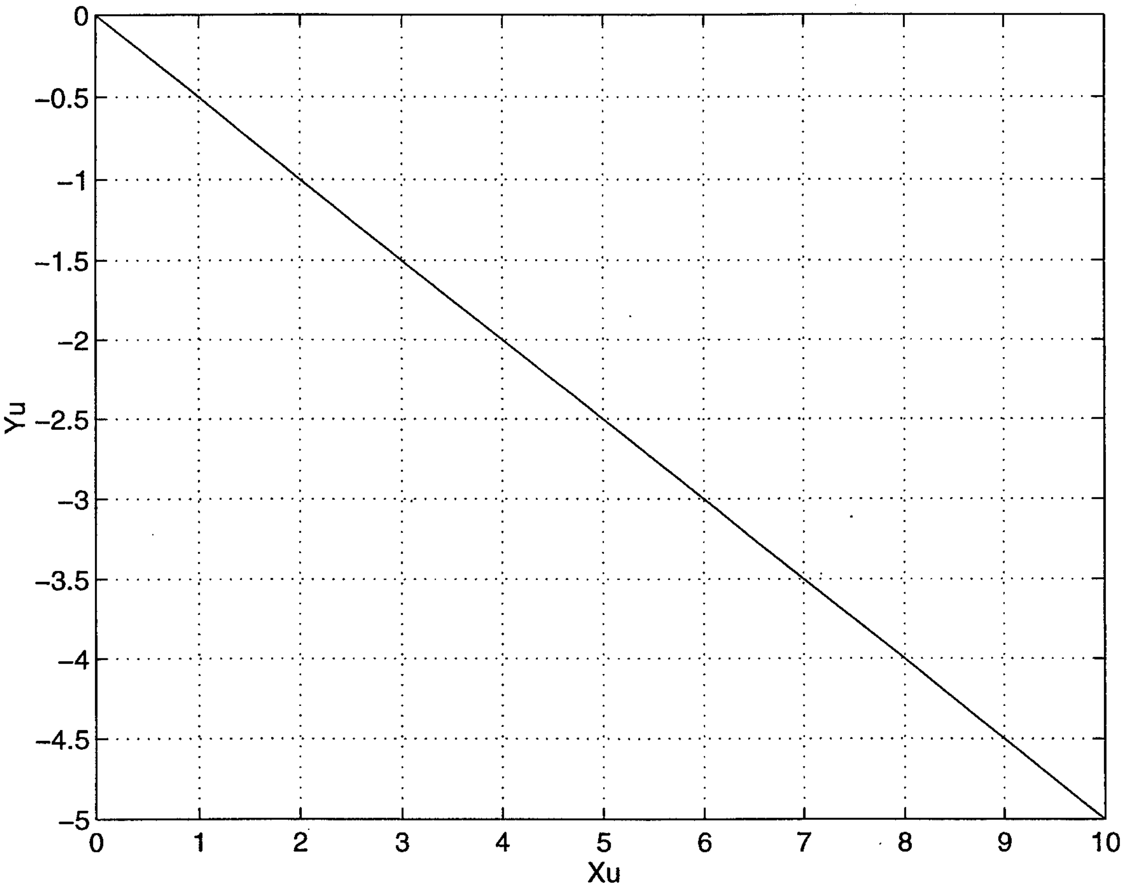

Figure 6: X-Y plot

B. INDEPENDENT CONTROL OF POSITION AND ORIENTATION

Figure 7 through Figure 14 show the response of the two wheel drivable vehicle compared to the one wheel drivable vehicle for the same initial and final conditions used in the test. It is evident from Figure 7 to Figure 14 that in either case, both the position and orientation converge to the goal. This confirms that the position and orientation can be independently controlled. However the manner in which they reach the goal differ significantly.

The vehicle with only one of the wheels drivable quickly accelerates and rotates early in the trajectory and then slowly approaches the goal. The vehicle with both wheels drivable has a steady velocity and rotation throughout the trajectory. This is especially evident in Figure 11 and Figure 12. The body angle versus time clearly show the differences between the two simulations, even though both trajectories follow a direct path to the goal.

Both the constant rate of speed and constant rate of rotation of the body would be highly beneficial if there were on board sensors scanning the environment during the journey.

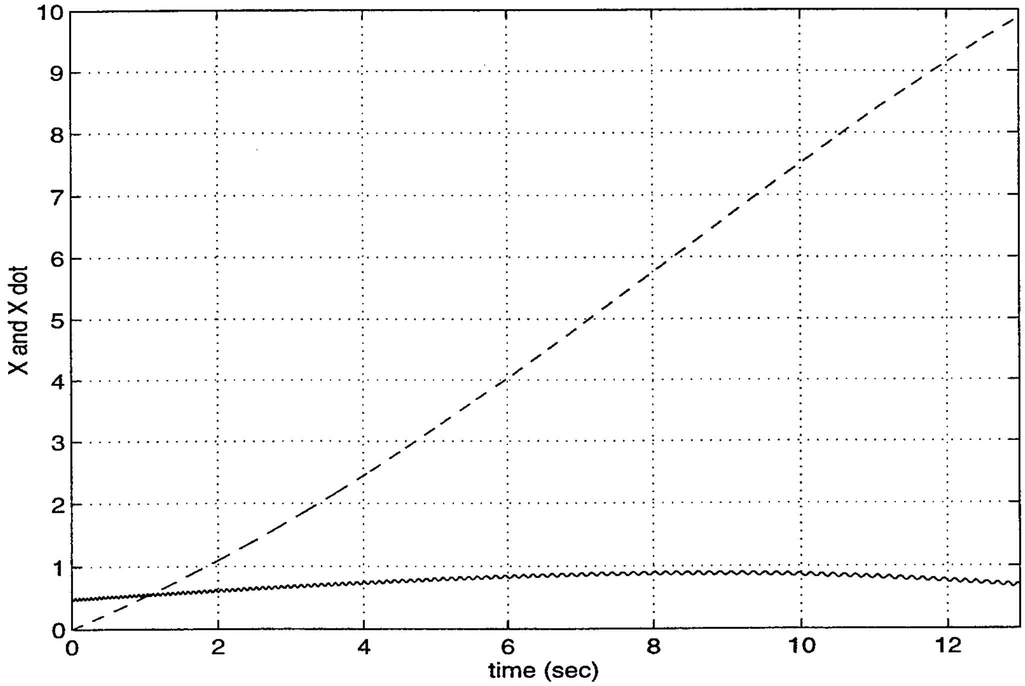

Figure 7: Two wheel drivable vehicle (X: dashed, X dot: solid)

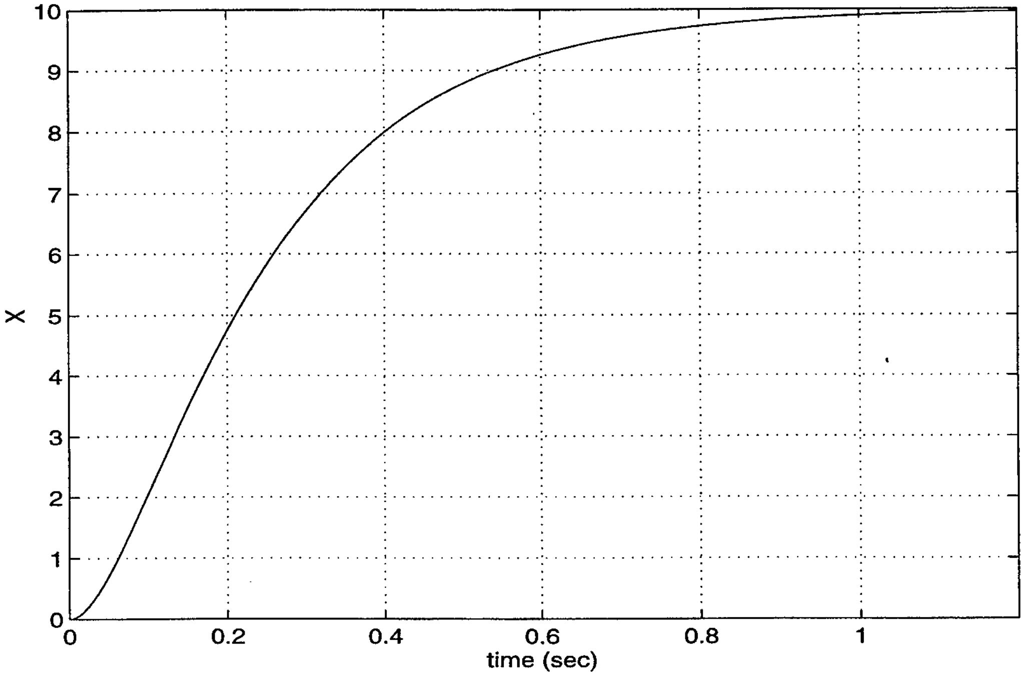

Figure 8: One wheel drivable vehicle, Xu versus time

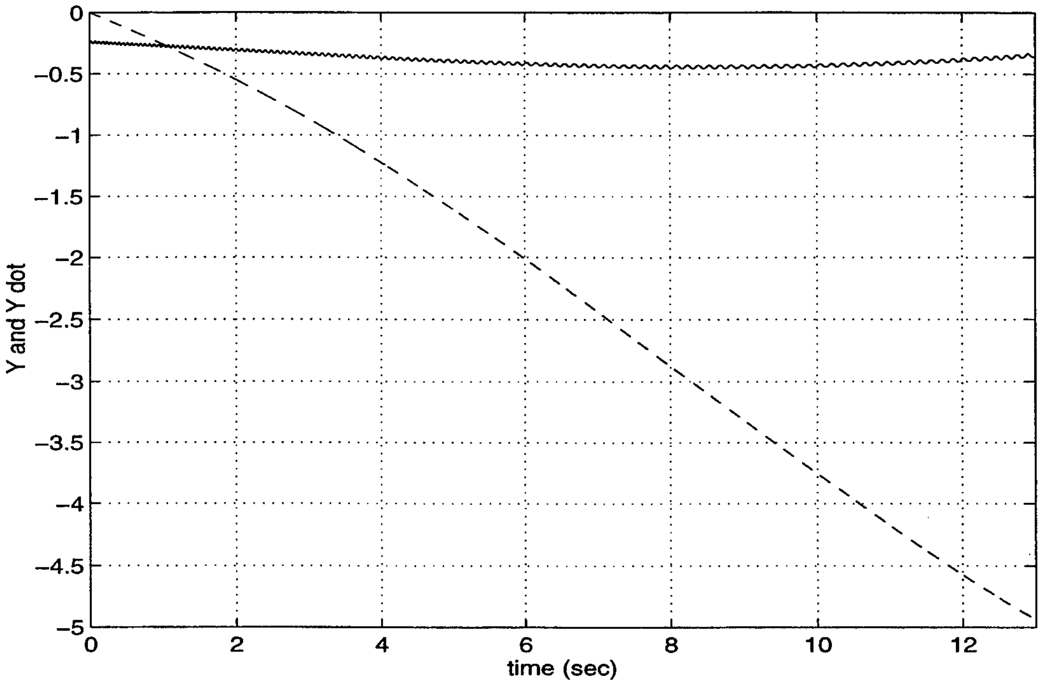

Figure 9: Two wheel drivable vehicle (Y: dashed, Y dot: solid)

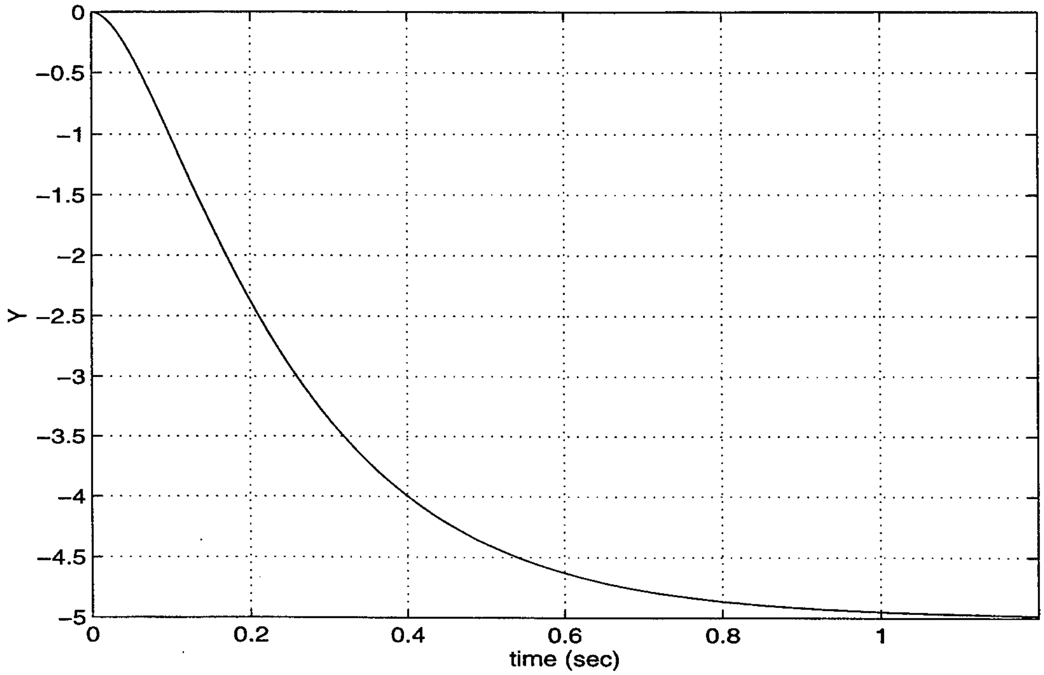

Figure 10: One wheel drivable vehicle, Yu versus time

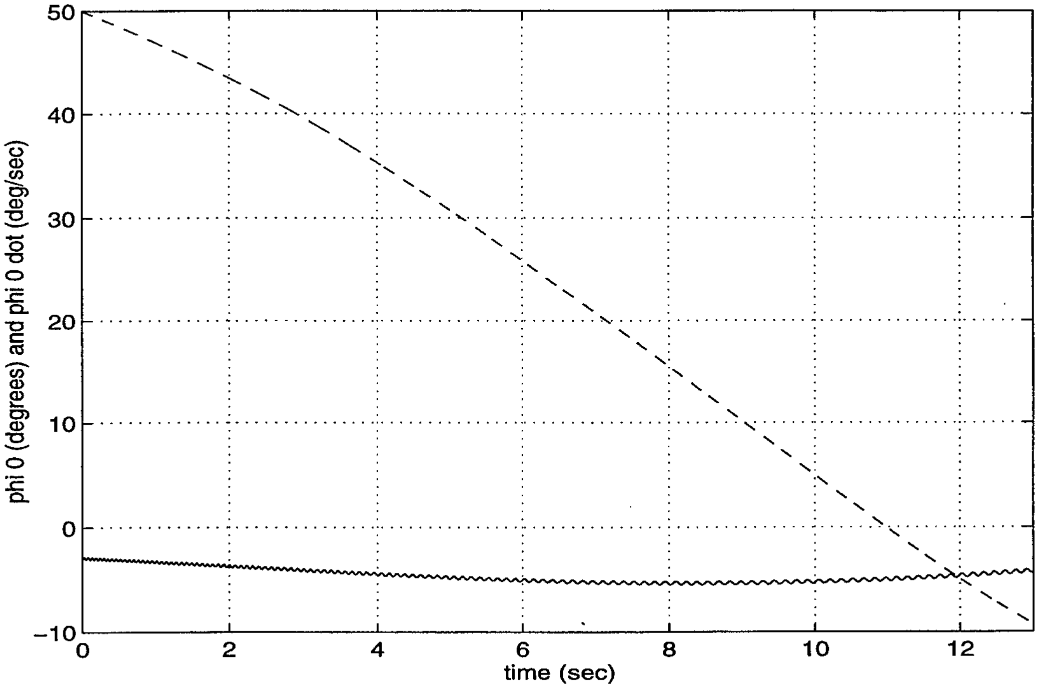

Figure 11: Two wheel drivable vehicle (phi: dashed, phi dot: solid)

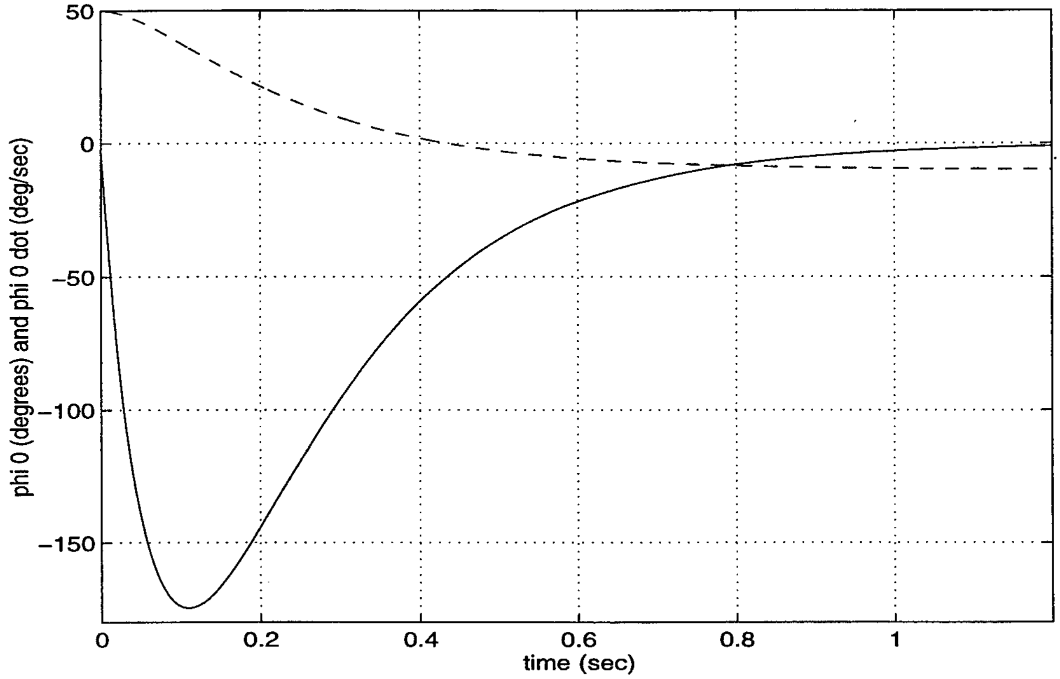

Figure 12: One wheel drivable vehicle (phi: dashed, phi dot: solid)

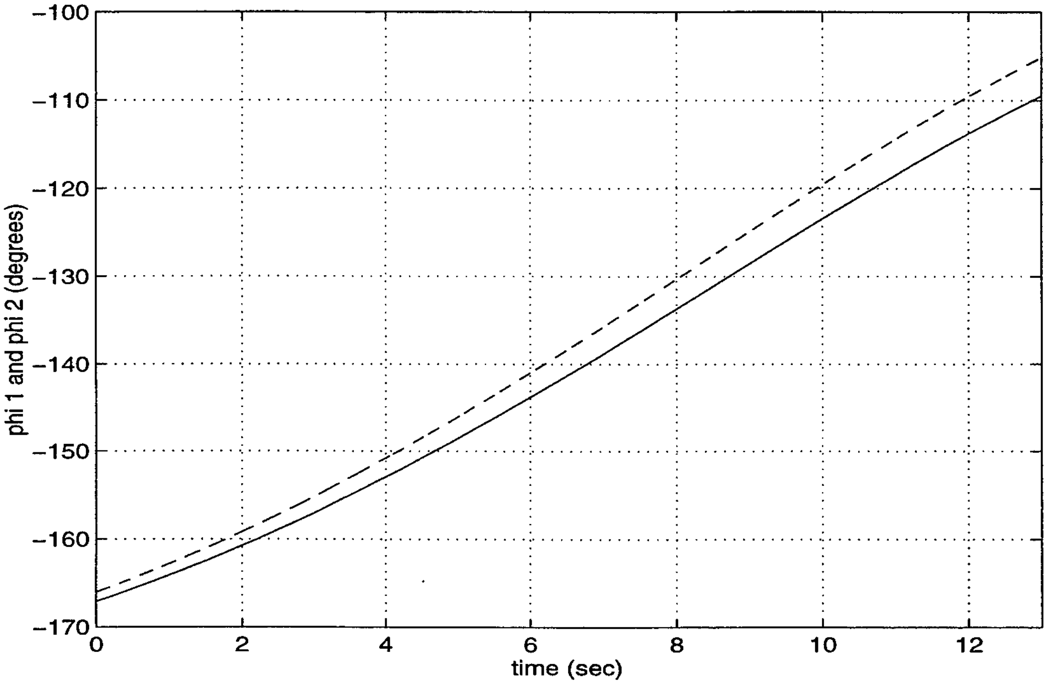

Figure 13: Two wheel drivable vehicle (phi 1: dashed, phi 2: solid)

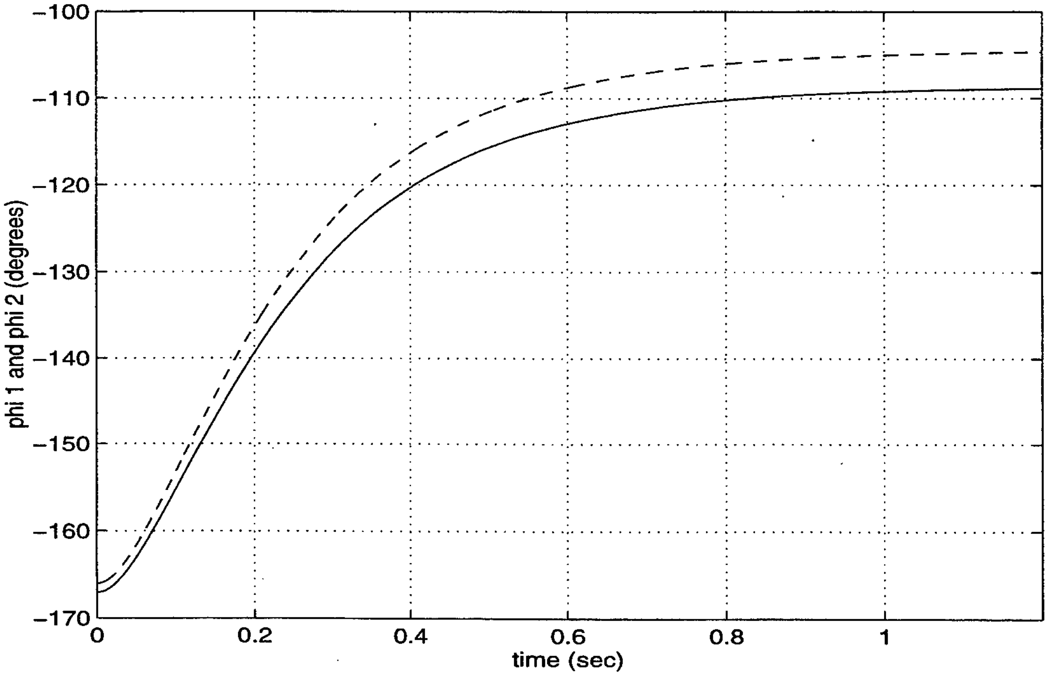

Figure 14: One wheel drivable vehicle (phi 1: dashed, phi 2: solid)

C. ONE WHEEL VERSUS TWO WHEEL DRIVABLE VEHICLES

Figure 15 and Figure 16 emphasize the differences between the one wheel drivable and two wheel drivable simulations. Even though both cases have two wheel steering, when both wheels are drivable, the transition from the initial starting point to the final goal point is much more linear than when only one wheel is powered. The body angle was adjusted by 90 degrees to the longitudinal axis of the vehicle, so that its orientation is from a more familiar perspective.

In Figures 15 and 16, each frame of the vehicle represents the vehicle's position, wheel angle, and the vehicles orientation at a particular point in time. Each snapshot is taken at equal intervals of time. These two figures clearly show that when only one wheel is being drivable it must approach the final goal point slowly to align to the correct orientation. When both wheels are drivable, the rotation of the vehicle is consistent throughout the trajectory.

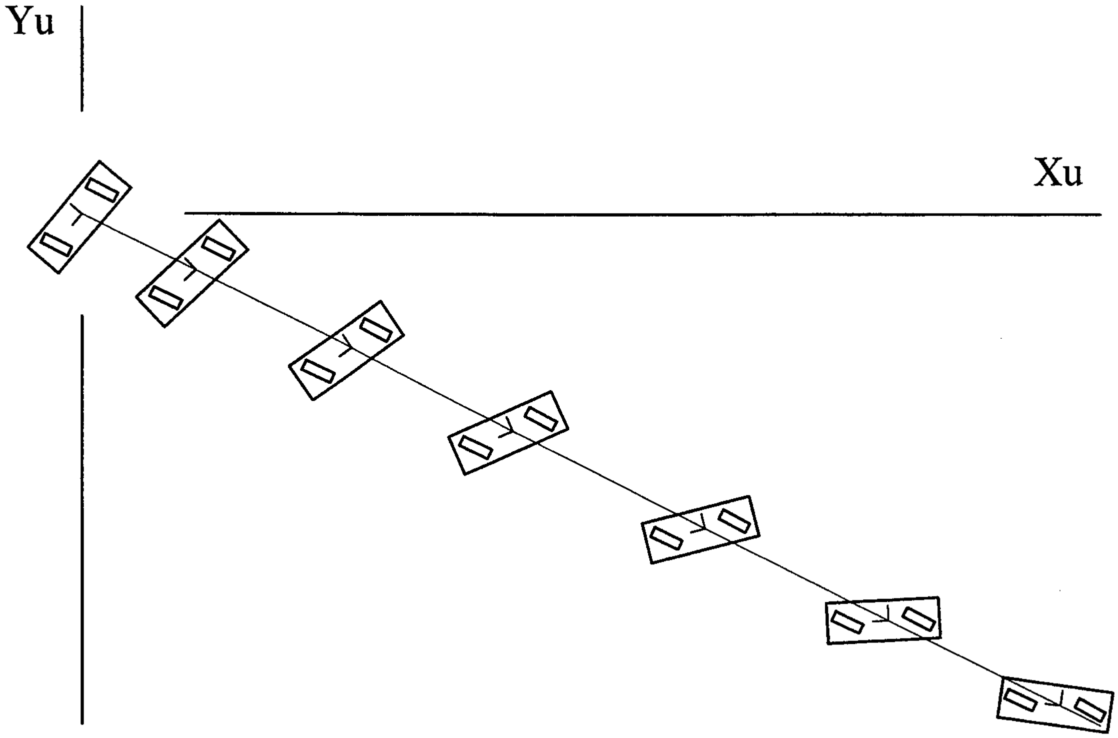

Figure 15: Two wheel drivable vehicle trajectory

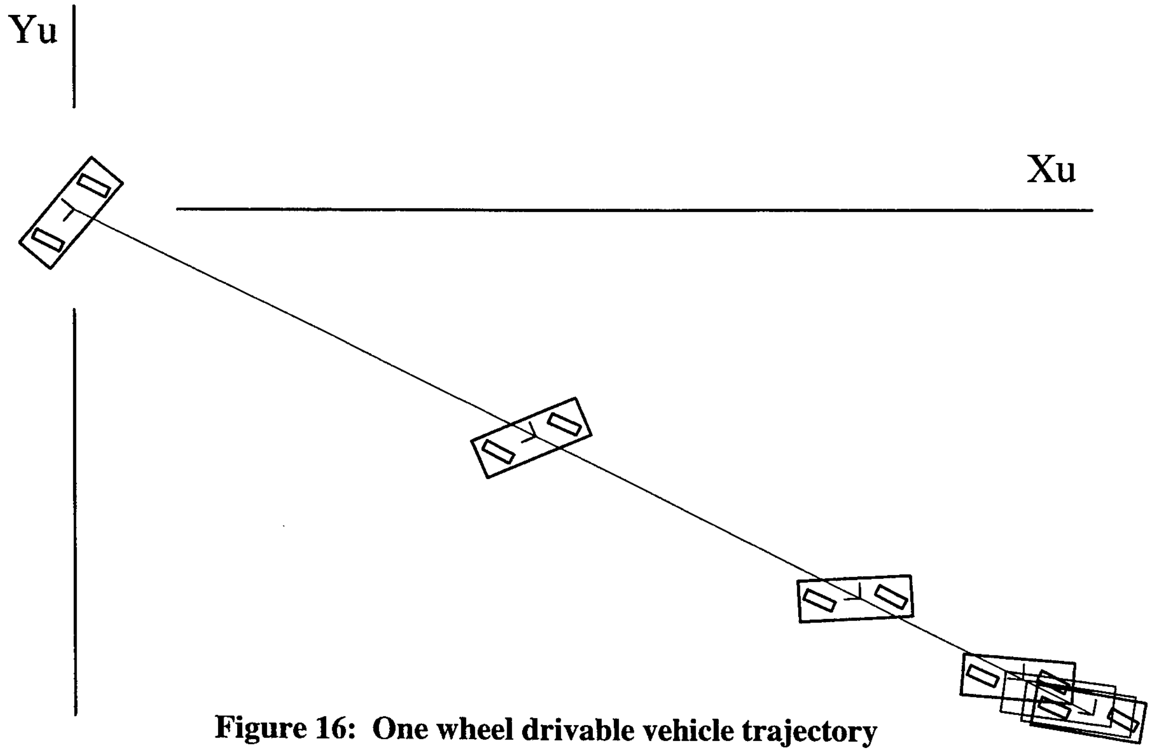

Figure 16: One wheel drivable vehicle trajectory

V. CONCLUSION AND FUTURE WORK

This thesis studied the control of a two-wheel vehicle with both wheels steerable and drivable. Unlike one-wheel steer mobile robots (e.g., the automobile/bicycle/tricycle type of mobile robots), the control of two-wheel steer robots are less intuitive and more difficult. By making both wheels drivable the complexity of the control algorithm increases further. Using a dynamic nonlinear feedback, independent control of the position and orientation of a mobile robot was obtained. The orientation is no longer an uncontrollable state variable governed by internal dynamics. Consequently, while the vehicle follows a direct path to its goal, its orientation does not have to be in the tangential direction of the path. For example, the orientation of the vehicle body can be independently controlled for scanning with onboard sensors.

Further work on this project includes:

The concept developed in this thesis can be extended to an all-wheel steering, all wheel drivable vehicle with four independent wheels. This may require redefining the constraint equations as well as the kinematic force and velocity equations may be required.

Distribution of the torque between the wheels would be greatly beneficial if one of the wheels began to slip. This simulation used a constant torque value for each wheel initially, but later trials found that a constant torque divided by the angular speed of the wheel squared provided the best overall performance. More research is needed on how exactly to distribute the torque to each wheel depending on the steering angle, final and initial position and configuration, and surface conditions.

It was stated from Equation (3) that the input velocities, η, were chosen arbitrarily. Perhaps better performance could be obtained from using the two angular wheel velocities and one steering angular velocity for the input parameters. These new inputs would make each input torque independent of the other, allowing one of the wheels to slip.

LIST OF REFERENCES

---

1. Nomadic Technologies, Inc., Nomad 200 user's guide, Technical report, 2133 Leghorn Street, Mountain View, CA 94043, 1993.

2. Yun, Xiaoping and Sarkar, Nilanjan, "Dynamic Feedback Control of Vehicles with Two Steerable Wheels," *Proceedings of 1996 IEEE International Conference on Robotics and Automation*, pp 3105-3110, Minneapolis, MN, April, 1996.

3. DeCorte, Celeste, Holland, John and Marin, Antonio, "Security robots - a dual-use technology," *Defense Electronics*, pp 19-2, September 1994.

4. Furukawa, Y., "A review of four-wheeled steering studies from the viewpoint of vehicle dynamics and control," *Vehicle System Dynamics*, pp 18(1-3):151-185, 1989.

5. Yu, Ssu-Hsin and Moskwa, J., "A global approach to vehicle control: Coordination of four wheel steering and wheel torque," *Journal of Dynamic Systems, Measurement and Control*, pp 116:659-667, December 1994.

6. Bushnell, L. G., Tilbury, D. M. and Sastry, S. S., "Steering three-input nonholonomic systems: The fire truck example," *International Journal of Robotics Research*, pp 14(4):366-381, August 1995.

7. Kanayama, Y., "Two dimensional wheeled vehicle kinematics," *Proceedings of 1994 International Conference on Robotics and Automation*, pp 3079-3084, San Diego, CA, May 1994.

8. Borenstein, J., "Control and kinematic design of multi-degree-of-freedom mobile robots with compliant linkage," *IEEE Transactions on Robotics and Automation*, pp 11(1):21-35, February 1995.

9. Novel, B. d'Andrea , Bastin, B., and Campion, G., "Dynamic feedback linearization of nonholonomic wheeled mobile robots," *Proceedings of 1992 International Conference on Robotics and Automation*, pp 2527-2532, Nice, France, May 1992.

10. Nijmeijer, H., and van der Schaft, A. J., *Nonlinear Dynamic Control Systems*, Springer-Verlag, New York, 1990.

---

11. The MathWorks, Inc., Simulink user's guide, Technical report, 24 Prime Park Way, Natick, MA 01760, 1995.

INITIAL DISTRIBUTION LIST

1.	Defense Technical Information Center 8725 John J. Kingman Rd., Ste 0944 Ft. Belvoir, VA 22060-6218	2
2.	Dudley Knox Library Naval Postgraduate School 411 Dyer Rd. Monterey, CA 93943-5101	2
3.	Chairman, Code EC Department of Electrical and Computer Engineering Naval Postgraduate School Monterey, CA 93943-5121	1
4.	Prof. Xiaoping Yun, Code EC/Yx Department of Electrical and Computer Engineering Naval Postgraduate School Monterey, CA 93943-5121	2
5.	Prof. Roberto Cristi, Code EC/Cr Department of Electrical and Computer Engineering Naval Postgraduate School Monterey, CA 93943-5121	1
6.	Lt. Douglas R. Gerrard 719 Nacional Court Salinas, CA 93901-4703	6